In vitro and *in vivo* characterisation of a novel peptide delivery system: amphiphilic polyelectrolyte-salmon calcitonin nanocomplexes

Woei-Ping Cheng [a], Colin Thompson [b], Sinéad M. Ryan [c], Tanira Aguirre [c], Laurence Tetley [d], David J. Brayden * [c]

[a] School of Pharmacy, University of Hertfordshire, College Lane Hatfield AL10 9AB, UK,
[b] School of Pharmacy and Life Sciences, The Robert Gordon University, Schoolhill, Aberdeen AB10 1FR, UK
[c] School of Veterinary Medicine and Conway Institute, University College Dublin, Dublin 4, Ireland
[d] Division of Infection & Immunity, IBLS, Integrated Microscopy Facility, Joseph Black Building, University of Glasgow, Glasgow G12 8QQ, UK

*Author for correspondence:
Email: david.brayden@ucd.ie
Tel.: +353 (1) 7166013
Fax: +353 (1) 7166219

Abstract

The cationic peptide, salmon calcitonin (sCT) was complexed with the cationic amphiphilic polyelectrolyte, poly(allyl)amine, grafted with palmitoyl and quaternary ammonium moieties at pH 5.0 and 7.4 to yield particulates (sCT-QPa). The complexes were approximately 200nm in diameter, had zeta potentials ranging from +20 to +50mV, and had narrow polydispersity indices (PDIs). Differential scanning calorimeter revealed the presence of an interaction between sCT and QPa in the complexes. Electron microscopy confirmed the zeta-size data and revealed a vesicular bilayer structure with an aqueous core. Tyrosine- and Nile red fluorescence indicated that the complexes retained gross physical stability for up to 7 days, but that the pH 5.0 complexes were more stable. The complexes were more resistant to peptidases, serum and liver homogenates compared to free sCT. *In vitro* bioactivity was measured by cAMP production in T47D cells and the complexes had EC50 values in the nM range. While free sCT was unable to generate cAMP following storage for 7 days, the complexes retained approximately 33% activity. When the complexes were injected intravenously to rats, free and complexed sCT (pH 5.0 and 7.4) but not QPa reduced serum calcium over 120 min. Free and complexed-sCT but not QPa also reduced serum calcium over 240 min following intra-jejunal administration. In conclusion, sCT-QPa nanocomplexes have been synthesised that are stable, bioactive and resistant to a range of peptidases. These enhanced features suggest that they may have the potential for improved efficacy when formulated for injected and oral delivery.

Key words:

Salmon calcitonin, poly(allyl)amine, amphiphilic polymers, oral peptide delivery, peptidase inhibition.

1. Introduction

Since complexation of bovine serum albumen (BSA) with a synthetic polyelectrolyte was first described [1], such complexes have been used widely in the food and biotechnology industry. Examples include stabilisation of enzymes for biosensors [2], and for developing protein separation methods [3]. Use of polyelectrolytes for non-injected peptide and protein delivery resulted in formulation of positively-charged chitosan nanocomplexes or hydrogels with insulin [4, 5], BSA [6], and catalase [7]. The principle mechanism of the non-covalent association is based on electrostatic interaction between positively-charged polymers and negatively-charged proteins to yield a polyelectrolyte complex. Most peptides and proteins however, typically exhibit amphiphilic character due to the presence of multiple hydrophobic and hydrophilic amino acid residues in the primary sequence. Amphiphilic polymers may have unique potential in peptide delivery due to their ability to interact with such peptides via both electrostatic and hydrophobic association. However, to our knowledge only a few groups have studied them for delivery of therapeutic peptides including insulin [8] and salmon calcitonin (sCT) [9].

Our previous work demonstrated the use of novel comb-shaped amphiphilic polyelectrolytes based on polyallylamine (PAA) designed for oral delivery of insulin [10-12]. PAA protected insulin from *in vitro* gastrointestinal enzymatic degradation by pepsin, and trypsin to an extent [12], due to the nature of the hydrophobic pendant group and the presence of quaternary ammonium moieties [10]. Among the amphiphilic polyelectrolytes examined, the most promising analogue was PAA grafted with a combination of palmitoyl (4.2% mole) and quaternary ammonium moieties (QPa, 73% mole). Proteins and peptides can be anionic or

cationic at physiological pH, depending on their isoelectric point (PI) and the pH of the compartment solution. Therefore, it is important to assess the ability of amphiphilic polyelectrolytes to deliver both cationic and anionic peptides. To date, most research has focussed on complexation between polymers and peptides of opposite charge. There are reports which suggest that polyelectrolyte complexation can indeed be formed with the same overall charge due to the presence of localized patches of opposite charge on the peptide surface [13], or due to hydrophobic interactions or hydrogen bonding between polymer and peptide [14].

The question for this current study was therefore whether PAA could be complexed with a cationic peptide while retaining physicochemical properties that are compatible with maintenance of bioactivity. sCT is a 32-residue calcium-regulating peptide hormone produced by parafollicular cells of the thyroid gland, which is used clinically as an adjunct anti-resorptive treatment for post-menopausal osteoporosis and also as a second line treatment for Paget disease [15]. Recent data suggests that sCT also has potential as a disease-modifying anabolic agent acting on osteoarthritic cartilage to promote collagen and proteoglycan synthesis [16]. Marketed sCT for osteoporosis is available as a nasal spray or as subcutaneous/intramuscular injections. An oral product would have patient acceptability advantages over both nasal sCT and oral bisphosphonates, the former prone to occasional local mild irritation due to the presence of permeation enhancers [17], while the latter elicits a range of intestinal side-effects in a cohort of patients [18]. Anionic sodium tripolyphosphate was recently complexed to sCT to form an ionic complex via electrostatic attraction and it had some oral efficacy in rats [19]. Here, complexation between the cationic QPa and cationic sCT was achieved in pH 5.0 and pH 7.4 buffers and the resulting nanocomplexes yielded positive outcomes from the standpoint of

physicochemical properties, resistance to enzymatic degradation, *in vitro* sCT bioactivity as well as *in vivo* hypocalcaemic efficacy in rats.

2. Materials and Methods

2.1. Materials

Poly(allylamine hydrochloride) (PAA) (Mw = 15 kDa), palmitic acid-N-hydroxysuccinimide ester (98%), sodium acetate, tris(hydroxymethyl) aminomethane (Tris) (≥99%) and Nile Red were all purchased from Sigma–Aldrich, UK. All solvents (HPLC grade) and glacial acetic acid were purchased from Fisher Scientific Chemicals, UK. sCT was purchased from PolyPeptide Laboratories (Denmark). The Parameter™ cAMP (EIA) kit was purchased from R&D systems, UK. Tissue culture reagents were obtained from BioSciences, Ireland. All other chemicals were of reagent grade. T47D cells were purchased from LGC Standards, UK.

2.2. Synthesis of QPa

In accordance with [10], PAA was reacted with palmitic acid-N-hydroxysuccinimide ester, based on molar feeds of 1:0.025 (PAA monomer: palmitoyl group) to obtain PAA grafted with palmitoyl-pendant groups (Pa). Quaternisation (Q) was carried out by reacting Pa with over a 1000 molar excess of methyl iodide to obtain quaternary ammonium compounds, QPa (Fig. 1). The novel amphiphilic polymers were characterised by elemental analysis and ^{1}H NMR and the results confirmed 4.2% mole palmitoylation and the palmotoyl graft [10, 11].

2.3. Preparation of sCT-QPa nanocomplexes

Complex preparation of sCT with QPa was carried out similar to our previous method using insulin [11]. Two buffers, Tris (pH 7.4) and acetate buffer (pH 5.0) were used to separately prepare sCT-QPa complexes. Tris buffer was made up of 0.1 M Tris: 0.01 M HCl (87:13 %

(v/v)), and the acetate buffer was composed of sodium acetate (0.871 gL^{-1}) and glacial acetic acid (0.216 gL^{-1}). Solutions (4 $mgmL^{-1}$) were prepared by sonicating the polymer in either buffer using a Soniprep 150® sonicator (MSE Ltd., UK) for 5 min at the maximum amplitude. sCT stock solutions (2 $mgmL^{-1}$) were prepared also in both buffers using gentle magnetic stirring. Equal volumes (2 mL each) of QPa and sCT solutions were added together and the sCT-QPa complexes were formed spontaneously after mixing. The solutions were then left at room temperature for 120 min and the pH values were re-checked before characterisation as described in Section 2.4 and 2.5.

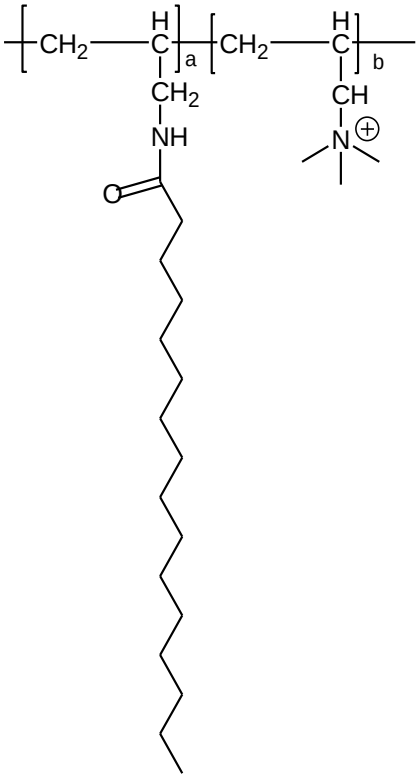

Fig. 1. Chemical structure of quaternary ammonium palmitoyl polyallylamine (QPa).

2.4. Characterization of polymer, sCT complexes

2.4.1. Differential scanning calorimetry (DSC)

QPa, sCT and QPa-sCT complexes (2:1 $mgmL^{-1}$) were freeze dried in a VirTis adVantage freeze drier (Biopharma Process Systems, UK) in both Tris and acetate buffers. Samples (1-2 mg) were then heated from $0^{o}C$ to $300^{o}C$ at $20^{o}Cmin^{-1}$ in a Q100 differential scanning calorimeter (TA instruments, UK), precalibrated with indium. The above experiment was repeated using sCT as received from the supplier.

2.4.2. UV Absorbance

The turbidity of QPa, sCT and sCT-QPa complexes were tested at day 0, 1 and 7 after preparation by taking absorbance readings at 350 nm using a Biomate 5 UV spectrophotometer (Thermo Spectronic, England) with a 1 cm quartz cuvette. Absorbance values were determined after blanking the spectrophotometer with the buffer used to prepare sCT/QPa samples. The samples were maintained at room temperature in the dark over the 7 days.

2.4.3. Intrinsic tyrosine fluorescence

The fluorescence of the tyrosine residues within sCT was measured using a LS 55 luminescence spectrometer (Perkin Elmer, USA) according to [20]. The changes of the emission spectra of the intrinsic tyrosine residues within the sCT give an indication of the physical stability of sCT. Emission spectra were recorded using the supplied software over an emission wavelength range of 290 to 400 nm after excitation at 274 nm using slit widths of 3 nm. An average of three scans was taken for each sample. Intensity values at peak emission wavelength were noted at days 0, 1 and 7 after the formation of sCT-QPa complexes and compared to free sCT.

2.4.4. Nile red fluorescence

Since intrinsic tyrosine fluorescence measurement may be less sensitive in detecting sCT aggregation compared to extrinsic fluorescence, extrinsic Nile red fluorescence was also used to determine sCT stability. QPa, sCT and sCT-QPa complexes were spiked with a 0.10 mM solution of Nile Red in ethanol (40 µL in 4 mL, n=3) [20]. Controls consisting of each buffer (4mL) were also spiked with Nile red. All samples were left in the dark at room temperature for the duration of the study. The emission intensities of the Nile red-spiked samples and nile red alone in each buffer were recorded between wavelengths of 600-700nm following initial excitation at 575 nm at a slit width of 7.5 nm. Peak intensities were measured using a LS 55 luminescence spectrometer (Perkin Elmer, USA) at days 0, 1 and 7 after sample preparation with an average of three scans of each sample.

2.4.5. Particle size analysis: photon correlation spectroscopy (PCS)

Hydrodynamic diameters and polydispersity indices (PDI) of polymer, sCT and sCT-QPa complexes in both buffers were determined using photon correlation spectroscopy (PCS) (Zetasizer Nano-ZS, Malvern Instruments, UK) at 25 °C. Analysis was carried out at days 0, 1 and 7 after preparation.

2.4.6. Zeta potentials

The zeta potential of QPa, sCT and sCT-QPa complexes were analysed using PCS (Zetasizer Nano-ZS, Malvern Instruments, UK) at days 0 and 7 after preparation. Prior to measurement, -50mV standards (Malvern Instruments, UK) were analysed; the data obtained agreed with that stated by the manufacturer.

2.4.7 Transmission electron microscopy (TEM)

Formvar/carbon-coated 200 mesh copper grids were glow-discharged and freshly-prepared complex solutions were dried to form a thin layer onto the hydrophilic support film. 1% aqueous methylamine vanadate (Nanovan®; Nanoprobes, Stony Brook, NY, USA) stain was applied and the mixture air-dried. The negatively-stained complexes were imaged with a LEO 912 energy filtering transmission electron microscope, at 80 or 100 kV.

2.5. In vitro and in vivo characterisation of sCT-QPa complexes

2.5.1. In vitro bioactivity: Intracellular cAMP elevation by sCT and complexes in T47D cells

cAMP-secreting activities of sCT and complexes were assessed using a T47D (human breast cancer cells) *in vitro* bioassay [21]. Human breast cancer cells (T47D) cells over-expresses calcitonin receptors and resulting in intracellular cAMP release upon activation by sCT. T47D cells were maintained in RPMI-1640 culture medium (Gibco) containing 1% penicillin–streptomycin (Gibco), 10% fetal bovine serum (Gibco) and insulin (0.2 IU/ml). The cells were plated at an initial density of 1.0×10^5 cells/well and incubated in a 95% air: 5% CO_2 atmosphere at 37 °C for 24 hours. Media was replaced with serum-free media and incubated for a further 24 hours. After washing with Hank's balanced salt solution (HBSS) (Sigma), cells were pre-incubated with the serum free media, supplemented with 0.2 mM 3-isobutyl-1-methyl-xanthine (IBMX) at 37 °C for 120 min. The cells were then incubated with different concentrations of freshly prepared (day 0) sCT and sCT-QPa (pH 5.0 and 7.4) complexes at 37 °C for 15 min. After removing the supernatants, intracellular cAMP was extracted from the cells by lysis and measured by ELISA (R&D Systems, UK). Concentration-response curves were also

carried out on samples from the same stocks after 7 days (day 7). The concentrations of sCT in the complexes were directly comparable with free sCT.

2.5.2. Intestinal enzyme metabolism

sCT-QP complexes were incubated with intestinal enzymes in transport buffer according to our previous description [22]: TPCK (N-p-tosyl-Lphenylalanine chloromethyl ketone)-treated trypsin (0.5 μM), TLCK (1- chloro-3-tosylamido-7-amino-2-heptanone)-treated chymotrypsin (0.1 μM) and elastase (0.48 μM). The concentrations of enzymes used were similar to those present in the gastrointestinal tract. Enzymes and substrates were incubated separately at 37 °C for 15 min, followed by co-incubation for 0, 15, 30, 45, 60 and 90 min. Samples were analysed for the capacity to induce cAMP production in T47D cells. Rate constants and half lives for formulations were calculated by assuming first order kinetics.

2.5.3 Hypocalcaemia of sCT-QPa formulations in rats: intravenous and intra-jejunal administration

Fasted male Wistar rats (300-350g) were initially anesthetised using intra-peritoneal (i.p.) injection of ketamine (75 mg/kg) and xylazine (10 mg/kg). Anaesthesia was maintained with isoflurane gas at the rate of 1.5 L/min mixed with O_2 (1 L/min) through a gas mask.
Rats were randomly divided into groups and were injected via the tail vein with 40 μg/kg (200 IU/mL/kg) sCT from each formulation: sCT, QPa, sCT-QPa, each prepared at both pH 5.0 and 7.4. Serum samples were obtained directly from the heart at time 0 and then at 15, 30, 60 and 120 min after i.v. injection. Intra-jejunal (i.j.) administration was also carried out in separate studies based on previous methods [23]. The proximal jejunum from anaesthetised rats were exposed after a midline laparotomy. 15 cm of jejunum was isolated by tighten the extremities up

with silk, taking care to avoid damage to blood vessels. Solutions containing 0.1mg/ml sCT (500 IU/ml) at the volume of 1ml/300g of bodyweight were instilled into the surgically exposed jejunal segments. The i.j. study had same design as for intravenous (i.v.) study, except that samples were withdrawn up to 240 min. Serum samples were analysed for calcium using a Randox Laboratory clinical chemistry colorimetric analyzer at a wavelength of 612 nm [22]. Animal experimental procedures adhered to the Principles of the Laboratory Animal Care, were performed in compliance with the Irish Department of Health and Children animal licence number, B100/4193, and were approved by the UCD Animal Research Ethics Sub-Committee.

2.6. Statistical analysis

R Statistical Language was used to perform non-linear regression, t-tests, Tukey-HSD *post hoc* ANOVA comparison and to construct confidence intervals. $P < 0.05$ was designated as the level of significance.

3. Results

3.1 Characterisation of sCT-QPa complexes

3.1.1. DSC

From the acetate samples, complexation led to a change in the DSC profile compared to free sCT and QPa alone. Free sCT had two endotherms, a broad endotherm at 70°C and another sharp endotherm at 130°C while QPa had endotherms at 90 and 240°C (Fig 2A). Upon complexation, the endotherms observed for free sCT had disappeared and a broad thermogram occurring at 120°C was observed. This result is consistent with our findings with the QPa-insulin complexes and other polyelectrolyte complexes [11,19]. The physical-chemical interaction between sCT and QPa had resulted in the disappearance of free sCT endotherms and the shift of QPa endotherm to a higher temperature.

In regards the Tris samples, the picture is more complex. QPa and the complex thermal profiles seemed to be very similar in acetate buffer, but not so in Tris. There was a large endotherm at 150^{o}C in the QPa Tris buffer sample that was not present in the acetate buffer sample, which may be due to the Tris itself having recrystallised on freeze drying (Fig 2B). The absence of this large peak in the thermal profile of QPa freeze-dried in water confirmed this hypothesis (data not shown). Complexation of QPa with sCT resulted in the disappearance of this peak and the small endotherms in the free sCT samples between 100-150^{o}C, suggesting the presence of an interaction between QPa and sCT. However, the multiple endotherms in the sCT and QPa samples between 225-250^{o}C were still present in the complex sample. This suggests possible degradation of QPa and/or denaturation of sCT in the complex at a high temperature. In Fig 2C, sCT as received from the commercial supplier had a different thermal profile compared to the free sCT freeze-dried in acetate or Tris buffer. The differences observed may

suggest that there is an interaction between sCT and the buffer. This may explain the lack of stability in Tris compared to acetate buffer, which was shown in our results (section 3.1.2, 3.1.3) as well as by others [20].

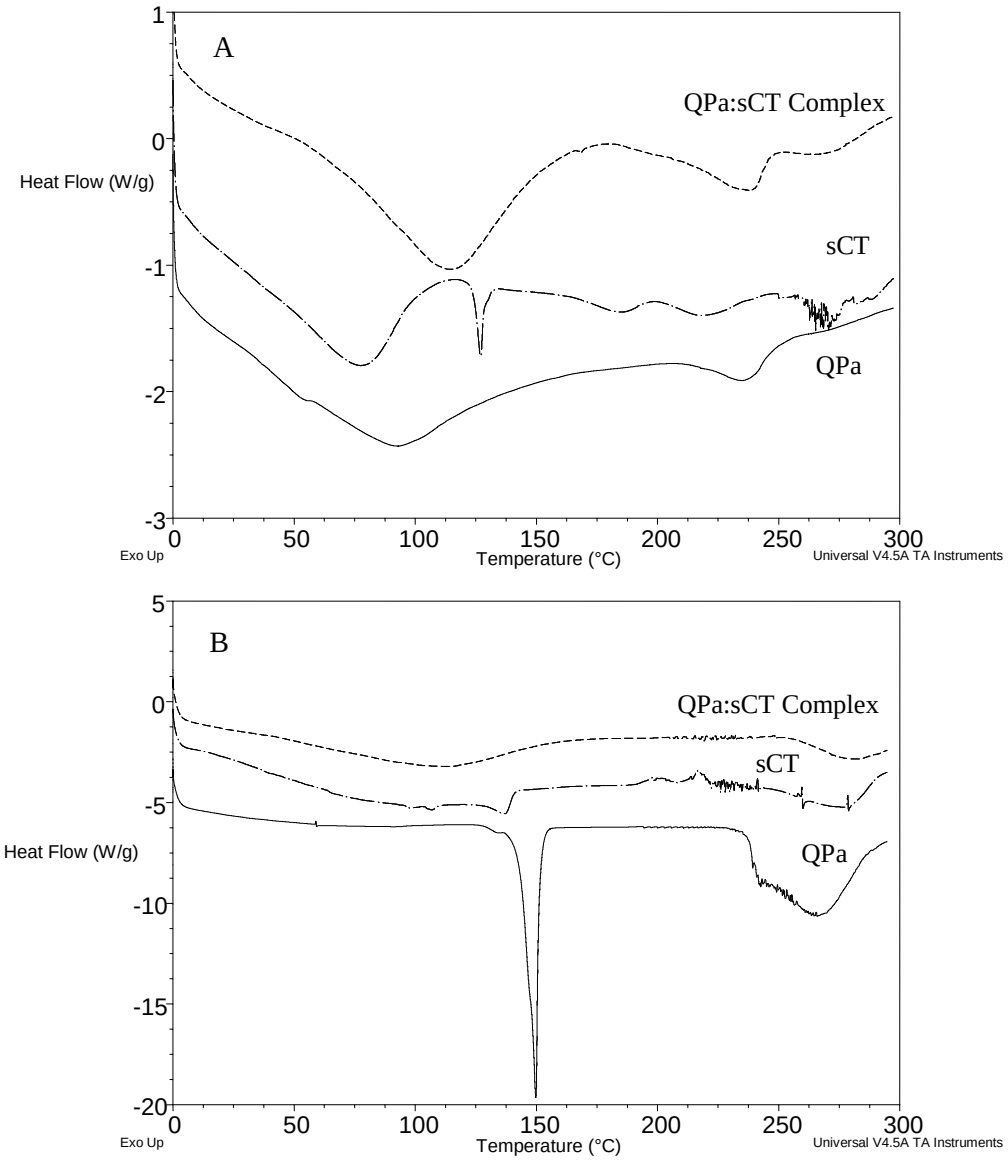

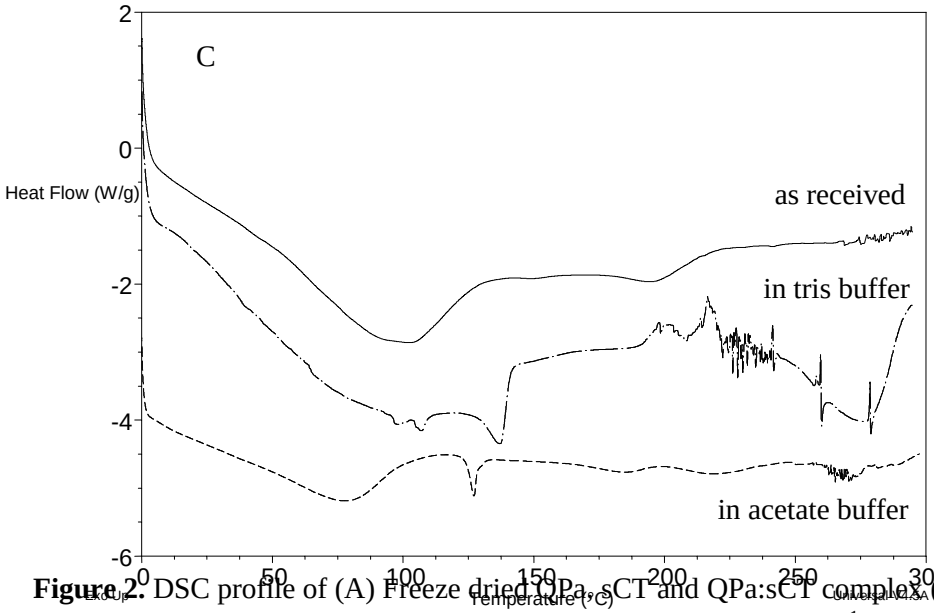

Figure 2. DSC profile of (A) Freeze dried QPa, sCT and QPa:sCT complex (2:1mgmL^{-1}) in acetate buffer. (B) Freeze dried QPa, sCT and QPa:sCT complex (2:1mgmL^{-1}) in Tris buffer. (C) freeze-dried sCT in acetate/ Tris buffer or as received.

3.1.2. PCS, zeta potential and UV spectroscopy

Samples were analysed for their hydrodynamic size, PDI, zeta potential and UV absorbance at day 0 and / or day 1 and at day 7 after preparation (Table 1). Samples were deemed stable at a gross level if absorbance readings remained below an O.D. value of 0-0.035 [20]. sCT samples were stable at day 0, but by day 7 absorbance values had risen above 0.035 in both buffers. This was particularly significant for samples at pH 7.4 (A=0.269) compared to pH 5 (A=0.044), suggesting that sCT was less stable at pH 7.4. The absorbance values for QPa alone were always above 0.035 as they were translucent. This meant that complex samples were also above 0.035. Again, however, samples appeared more stable at pH 5 than pH 7.4, given the smaller changes in absorbance at day 7; absorbance increased from 0.054 to 0.071 and from 0.053 to 0.253 at pH 5 and 7.4, respectively (Table 1). The precipitation observed for both sCT

and the complex at pH 7.4 at day 7 would suggest that the complex became unstable at this pH, although precipitation from the complex appeared to be less than from free sCT. It would have been expected that if the sCT and QPa were not interacting with each other, two distinct size populations would be present in the complex samples which would be indicated by higher size and PDI values and multiple peaks in the size distribution graph. However, all complex samples over 7 days had diameter and PDI values of less than 230 nm and 0.3 respectively (Table 1). In addition, one single peak was obtained in the size distribution graphs (Fig 2A, B), suggesting that complexation between sCT and QPa led to formation of compact nano-aggregates with relatively narrow size distribution at either pH. This suggests the absence of free sCT in the complexes, consistent with previous SEC-HPLC data from insulin-QPa complexes [11, 12]. Diameters and PDI values for sCT-QPa complexes were comparable to those of QPa, but differed markedly from those of sCT. Free sCT had a substantially higher hydrodynamic size ranging from 458nm to 2µm with a PDI of 1, indicating the presence of particulates of a wide diameter range.

Table 1. Size, zeta potential and absorbance of sCT, sCT-QPa in pH 5.0 or Tris buffers

	Day	***Hydrodynamic***	***PDI***	***Zeta Potential***	***Absorbance***

		diameter (nm)		*(mV)*	*(350 nm)*
pH 5.0					
sCT	0	458 (141)	0.527 (0.093)	39.1 (2.54)	0.000
	7	2471 (934)	1.000 (0.000)	20.8 (2.70)	0.044
QPa	0	226 (2)	0.201 (0.015)	52.5 (0.92)	0.060
	7	169 (4)	0.262 (0.003)	52.7 (1.17)	0.086
sCT-QPa	0	226 (7)	0.232 (0.029)	56.6 (0.88)	0.054
	1	227 (4)	0.228 (0.039)	n/a	0.059
	7	226 (5)	0.209 (0.031)	52.1 (1.09)	0.071
pH 7.4					
sCT	0	1827 (1279)	0.763 (0.191)	17.9 (0.78)	0.004
	7	1339 (190)	0.802 (0.148)	4.5 (0.26)	0.269
QPa	0	204 (2)	0.227 (0.008)	44.0 (2.07)	0.045
	7	128 (3)	0.177 (0.008)	40.7 (3.66)	0.066
sCT-QPa	0	197 (4)	0.206 (0.019)	44.7 (0.71)	0.053
	1	194 (4)	0.203 (0.014)	n/a	0.056
	7	225(18)	0.293 (0.044)	49.6 (2.00)	0.253

N= 3 ± SD for each parameter

All samples had positive zeta potentials ranging from +21 mV to +50 mV, apart from free sCT at pH 7.4 at day 7 (Table 1). However, zeta potential values for sCT-QPa complexes were much higher than those of free sCT, but were similar to those of QPa alone. The zeta potential graphs of complexes in both pH 5 and pH7.4 buffers showed a single peak appearing at

+57 mV and + 45mV respectively (Fig 3C, D), and these values were relatively constant after 7 days (Table 1).

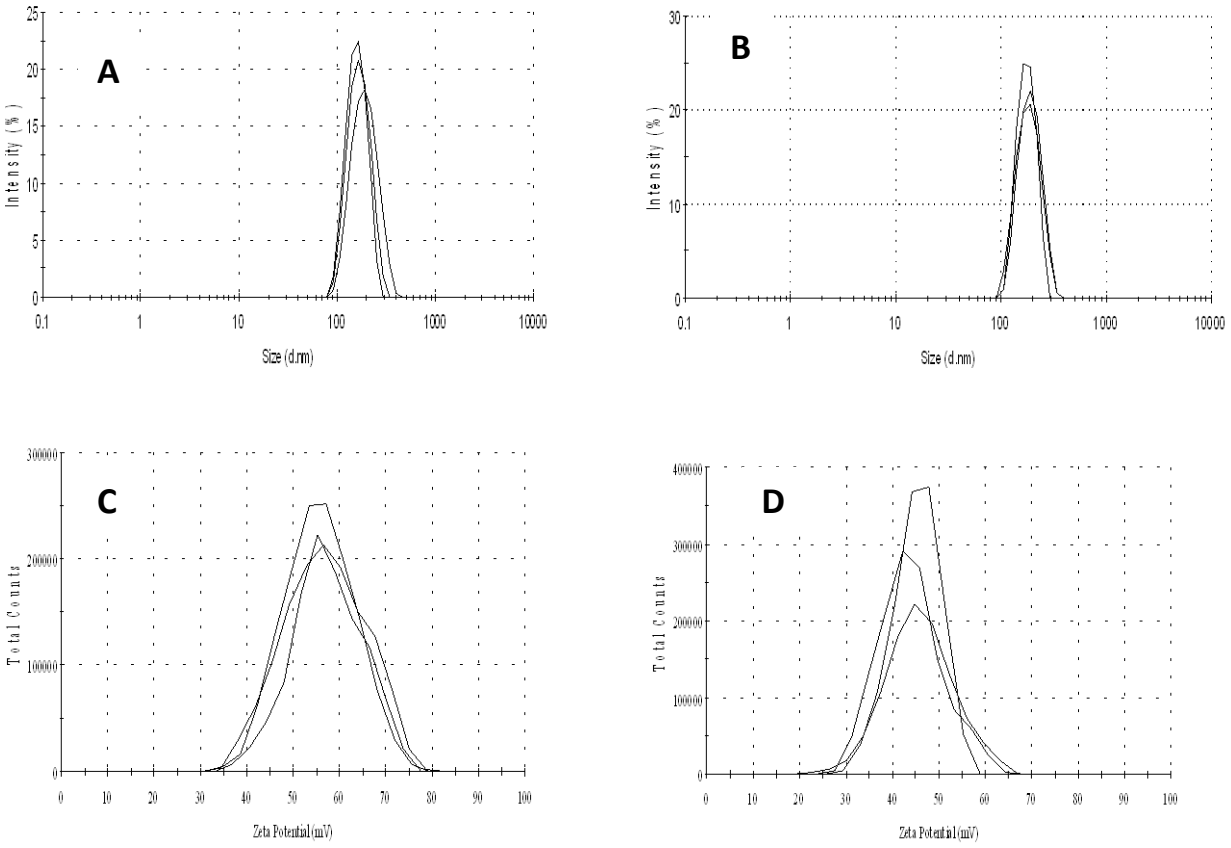

Fig. 3. Size distribution complexes at day 0 at pH 5.0 (A), and pH 7.4 (B). Zeta potential distribution of complexes at day 0 at pH 5.0 (C), and pH 7.4 (D) (triplicate samples).

3.1.2. Intrinsic tyrosine fluorescence

Intrinsic tyrosine fluorescence was measured in order to further assess stability of sCT in the complexes. The emission maxima wavelength should not change over time as it is intrinsic to tyrosine unless aggregation or fibril formation occurs. Stable sCT samples should not lose/gain less than 6 % of their peak intensity between days 1 and 7 [24]. There was little change in

$\lambda_{emission}$ and peak intensities for most of the samples over the period (Table 2). Both the sCT-QPa (pH 5.0) complexes and sCT alone (pH 5.0) remained stable and peak intensities only altered by 2.6 % and 1.8 %, respectively. However the intensity of the sCT-QPa complexes (pH 5.0) fell by 6.5 % and the sCT (pH 7.4) fell by 46.6 % at day 7. This would suggest that sCT is more stable at pH 5 than pH 7.4 and that complexation has a stabilizing effect on sCT at pH 5.0. QPa samples had negligible emission changes (data not shown).

3.1.3 Nile red fluorescence

sCT samples spiked with Nile red were considered stable if they had emission λ_{max} values > 630 nm [20]. Small changes in intensity were considered to be due to fluctuations in temperature and binding of Nile red to sample containers. Nile red has an emission maximum of 645 nm and the fall in maximum to 620-631 nm is a blue shift [20]. In contrast to tyrosine fluorescence, all Nile red spiked samples underwent shifts in emission λ_{max} (Table 3). Free sCT samples displayed minimal fluorescence (Table 3) as did Nile red alone in both buffers (data not shown). QPa itself also underwent a blue shift in the λ_{max}, while sCT-QPa complexes (pH 5.0 and 7.4) also exhibited blue shifts (Table 3). Given the shift in emission λ_{max} of the complexes was below 630 nm it would appear that they were less stable than sCT alone. However this greater shift may be due to the combined effect of QPa and sCT interaction with Nile red.

Table 2. Tyrosine fluorescence measurements of sCT and QPa, sCT complexes in pH 5.0 and pH 7.4 buffers (triplicate samples).

pH 5.0	*Day*	*Emission λ_{max} (nm)*	*Intensity at maximum*
sCT	0	307	503
	1	305	513
	7	305	504
sCT-QPa	0	306	486
	1	306	516
	7	306	503

pH 7.4	*Day*	*Emission λ_{max} (nm)*	*Intensity at maximum*
sCT	0	303	443
	1	304	434
	7	306	232
sCT-QPa	0	305	478
	1	304	513
	7	305	480

Table 3. Fluorescence of Nile red (1 µM)-spiked sCT, QPa and sCT-QPa QPa complexes and in pH 5.0 and pH 7.4 buffers.

pH 5.0	*Day*	*Emission λ_{max}, (nm)*	*Intensity at maximum*
sCT	0	630	2
	1	637	1.5
	7	637	1.8
QPa	0	631	232
	1	632	203
	7	632	144
sCT-QPa	0	626	172
	1	626	165
	7	626	164

pH7.4	*Day*	*Emission λ_{max}, nm*	*Intensity at maximum*
sCT	0	640	3.3
	1	637	1.9
	7	641	3.7
QPa	0	626	196
	1	628	171
	7	627	172
Complex	0	620	181
	1	620	173
	7	620	175

3.1.4. TEM

sCT did not form any discernable structures in either buffer when analysed using TEM (data not shown). The diameters of the sCT-QPa complexes at the two different pH values were approximately 120nm and the morphology of both complexes was similar; both appeared to be vesicular structures with aqueous cores (Fig. 4). The thickness of the vesicle was around 22nm, thicker than the typically reported bilayer membrane thickness of 11nm [24], indicating the membrane might consist of more than one bilayer.

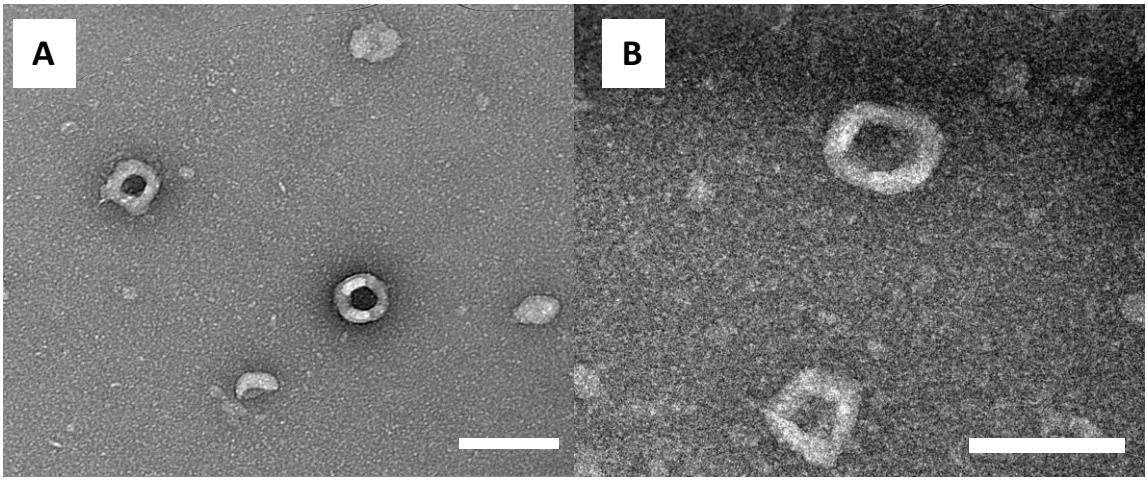

Fig. 4. Negatively-stained TEM images of freshly-prepared sCT-QPa complexes (2:1 mg mL^{-1}) in pH 5 buffer (A) or pH 7.4 buffer (B). Scale bar = 200 nm.

3.2. Intracellular cAMP induced by sCT and sCT-QPa on T47D cells

Intracellular cAMP activities in T47D cells were monitored to determine the bioactivity of sCT in freshly prepared complexes. Samples increased the intracellular cAMP in a concentration-dependent manner (Fig. 5A). Complexes in both buffers as well as free sCT were bioactive and maximal efficacy was achieved by each of the three groups. The EC_{50} values were (nM): free sCT (0.73 ± 0.1), sCT-QPa, pH 7.4 (3.3 ± 0.1) and sCT-QPa at pH 5.0 (7.9 ± 0.1). Although the EC_{50} values suggested that the presence of QPa in the complexes at pH 7.4 and pH 5.0 caused reductions in respective potency compared to free sCT, these nM values were still

very acceptable. The sCT bioactivity of the freshly prepared samples at day 0 and at day 7 following storage at room temperature in the dark was also determined (Fig 5B). Irrespective of the buffers used, free sCT was completely degraded at day 7, but there was still significant bioactivity in the complexes stored for 7 days.

A

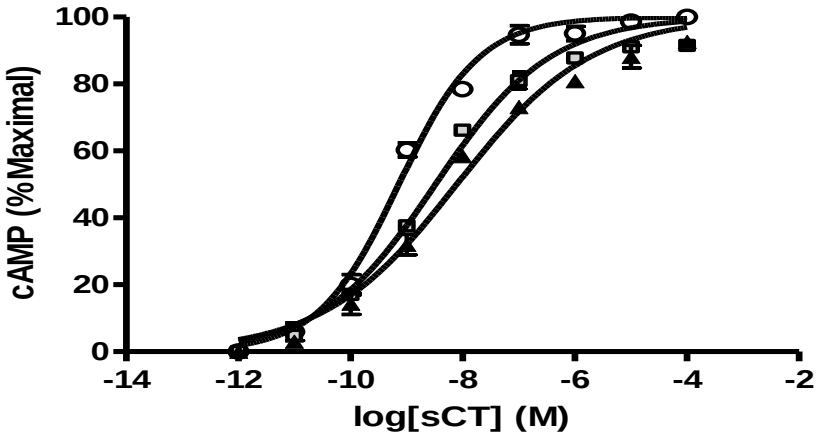

B

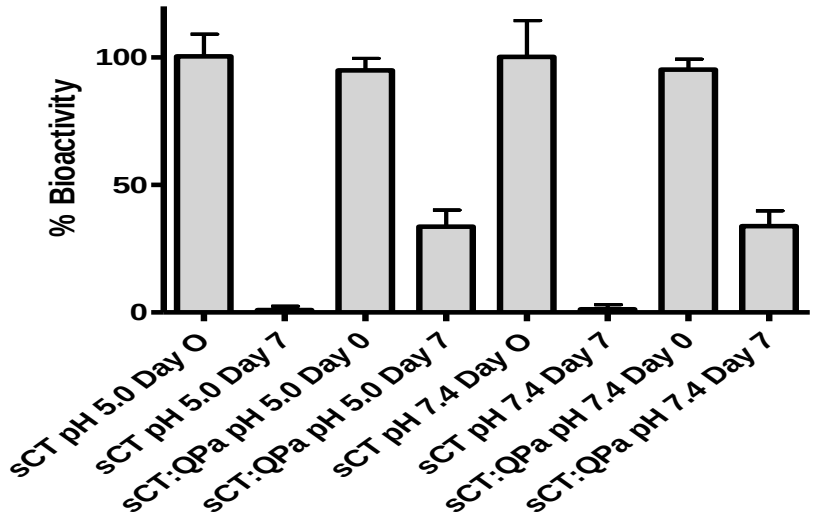

Fig. 5. A. Concentration-response curves for sCT and sCT-QPa stimulation of cAMP production in T47D cells. sCT (○), sCT-QPa, pH 7.4 (□), sCT-QPa, pH 5.0 (▲). B. cAMP

production by sCT and sCT-QPa complexes at pH 7.4 and pH5.0 on Day 0 and Day 7 on T47D cells. The concentration of sCT was 10µM in each preparation. (N=3 in each case).

3.3. Intestinal enzyme metabolism

Freshly prepared free sCT and sCT-containing complexes were incubated with three intestinal enzymes and the intracellular cAMP activities in T47D cells were determined. Free sCT was rapidly degraded by chymotrypsin, elastase and trypsin. There was only 3% activity remaining in the free sCT when exposed to all three enzymes combined at 30 min (Fig 6). At both pH values, the sCT in the complexes was significantly protected from degradation by the enzymes.

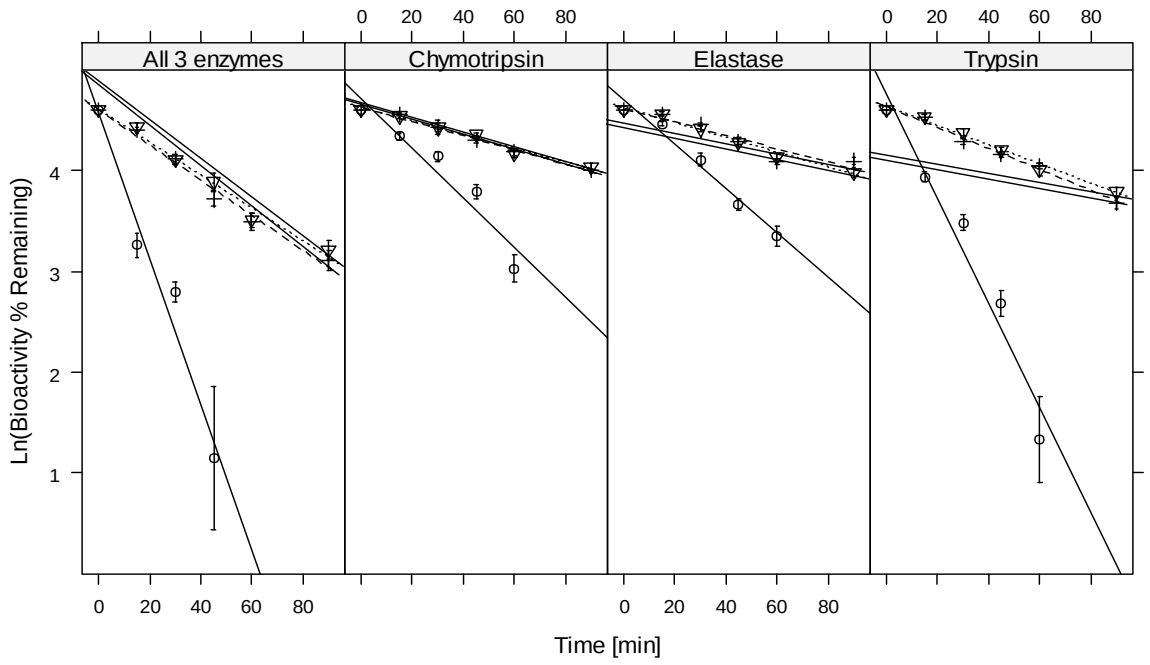

Figure 6: Degradation profiles of sCT, sCT-QPa (pH 5.0) and sCT-QPa (pH 7.4) when incubated with three intestinal enzymes. Samples were applied onto T47D cells and cyclic AMP measured. sCT (○), sCT-QPa, pH 7.4 (▽), sCT-QPa, pH 5.0 (+). Curve fitting was based on first order kinetics (N=3 in each case).

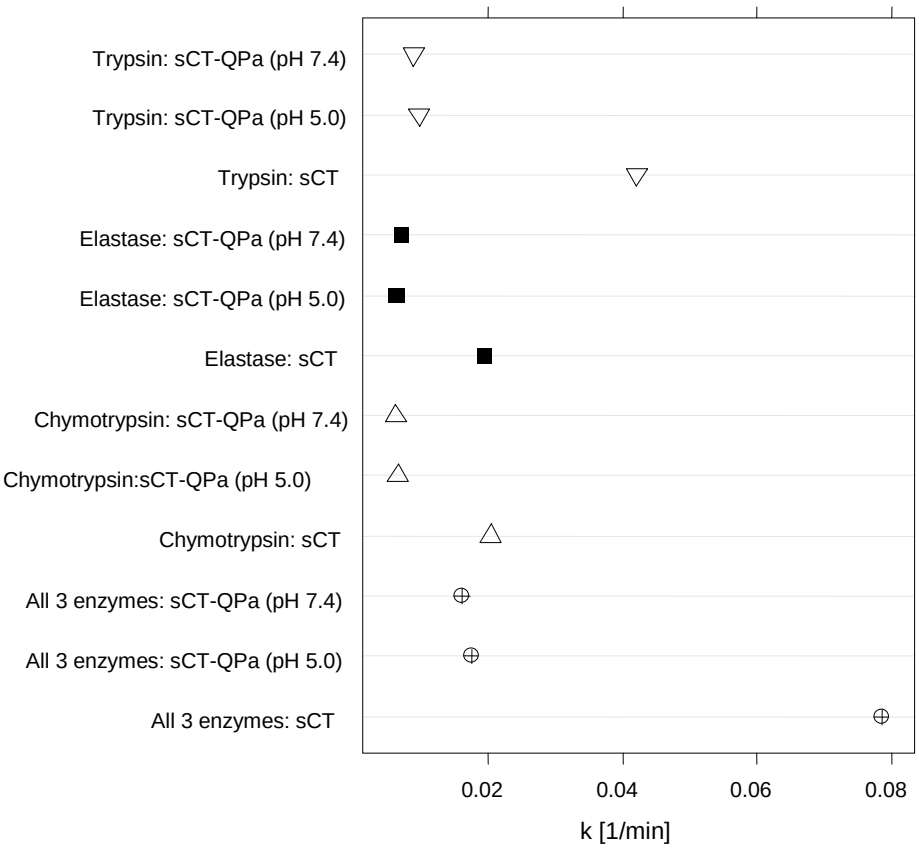

Fig. 7 Comparison of degradation rates of sCT, sCT-QPa (pH 5.0) and sCT-QPa (pH 7.4) in the presence of serine proteases, as determined by cyclic AMP measurements in T47D cells.

63.0 ± 0.1%, 57.0 ± 0.1% and 41.9 ± 0.02% bioactivity remained following sCT-QPa exposure to chymotrypsin, elastase and trypsin respectively for 90 min, pooled data at both pH values. QPa presence in both formulations reduced the degradation rate of sCT by 5-fold when all three enzymes were combined compared to free sCT (Fig 7) ($p < 0.005$).

3.4. Hypocalcaemia induced by sCT-QPa complexes in rats

The biological effects of sCT-QPa complexes at pH 5.0 and pH 7.4 were evaluated by induction of hypocalcaemic response in rats following i.v. and i.j. administration. At sCT equivalent doses following i.v. administration, the total percentage calcium decrease induced by

sCT (pH 5.0) and sCT-QPa (pH 5.0) were similar, 23.1 ± 2.3% and 22.9 ± 3.8% at 120 min respectively (Fig. 8A). sCT (pH 7.4) and sCT-QPa (pH 7.4) induced decreases of 30.0 ± 2% and 29.3 ± 1.7% respectively over the same period. There were no differences between any of the sCT preparations. QPa (pH 5.0 and 7.4) was without effect over the period following i.v. administration. A very similar set of data was obtained following i.j. administration (Fig. 8B). The sCT-QPa complexes were bioactive *in vivo* with no loss of activity compared to free sCT. Intestinally instilled complexes retained the capacity to cross the epithelium.

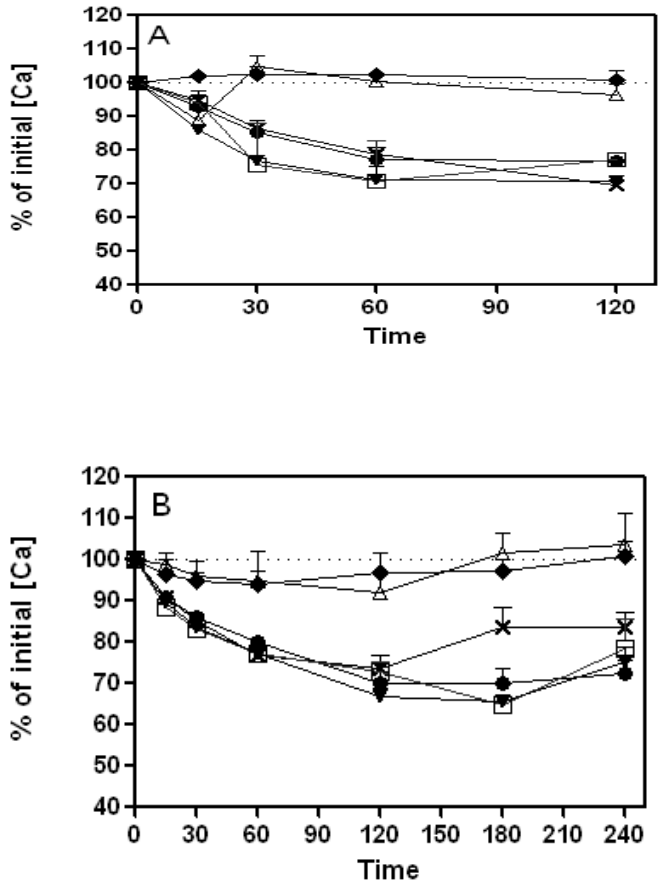

Fig.8. A. Plasma calcium levels in rat serum after i.v. administration of QPa, pH 5.0 (Δ), QPa, pH 7.4 (♦), sCT, pH 5.0 (●), sCT, pH 7.4 (x), sCT-QPa, pH 5.0 (□), and sCT-QPa, pH 7.4 (▼). Mean ± SEM (n = 3). B.i.j administration: groups and symbols as in A. (N = 3-4).

4. Discussion

There are four commercially available formulations of sCT; the recommended dose for the daily nasal spray to treat post-menopausal osteoporosis is 200 I.U, while 100 I. U. are administered every other day for injections. sCT is normally formulated in acidic media consisting of acetate, hydrochloric acid or citric acid buffers, as sCT is more stable in acid pH than at pH 7.4 [25]. Since the isoelectric point of sCT is 10.2, it will be positively-charged at acidic and physiological pH values [26]. We looked at the ability of the cationic amphiphilic polyelectrolyte (QPa) to complex with sCT at pH 5.0 and 7.4 and assessed the impact of the polymer on sCT's physical stability, resistance *in vitro* enzymatic degradation and *in vitro* and *in vivo* bioactivity. We did not expect complexation to occur easily in view of the likely potential for electrostatic repulsion.

Polyamines are effective non-cytotoxic permeation enhancers across intestinal epithelia and they can open epithelial tight junctions *in vitro* [27]. For example, spermine formulated in polyacrylic acid polyelectrolyte complexes improved the oral absorption of sCT in rats following intra-duodenal administration [28]. It is possible that QPa may also act as an epithelial permeation enhancer and this may be of benefit in addition to peptidase inhibition. Initial studies suggest that it also reversibly opens tight junctions in Caco-2 monolayers (unpublished data). We have previously illustrated the potential use of amphiphilic polyamines based on PAA for oral insulin delivery [11, 12]. The attachment of palmitoyl chains and the addition of quaternary ammonium moieties resulted in an 11-fold reduction in cytotoxicity of QPa compared to its parent molecule (PAA), Although sCT is positively charged, complexation was still achieved with QPa in the current study, resulting in a narrow particle size distribution with a hydrodynamic diameter of approximately 200nm. Unlike other polyelectrolyte complexes,

which require centrifugation to obtain the nano-complexes, freshly prepared sCT-QPa complexes were clear in appearance, confirmed by the low absorbance UV reading and the absence of pellets after centrifugation. The differences observed between the DSC thermal profiles of free sCT and complexes in both pHs suggesting the presence of physical-chemical interaction between sCT and QPa, which correlated well with other polyelectrolyte-protein complexes [11,19]. The assessment of the physical stability of the complex was based on data from the combination of size and zeta potential measurements, turbidity, as well as intrinsic and extrinsic fluorescence. Overall, QPa complexation had a positive effect on the physical stability of sCT. Unstable formulations would have resulted in an increase in particle size, turbidity and peptide aggregation. While free sCT was more physically stable for longer periods at pH 5.0 than pH 7.4 according to the tyrosine fluorescence study, the *in vitro* bioassay suggested little difference at the level of function where both very equally efficacious at Day 0 and inefficacious at Day 7. Although sCT-QPa (pH 7.4) complexes showed some signs of instability at 7 days, the changes detected by these studies were considerably less than the deterioration in free sCT (pH 7.4) over the same period.

Nile red can detect hydrophobic micro-domains in aqueous solutions formed by amphiphilic polymers [29]. The blue shift in the maximum emission wavelength observed with QPa correlates with the results with alkylated poly(L-lysine) citramide [29]. Thus, it partitions from the aqueous environment into the hydrophobic domains formed by the palmitoyl grafts on QPa. Importantly, a similar blue shift was also observed in free sCT (pH 5. 0), indicating the presence of hydrophobic domains on the peptide. Finally, when sCT was complexed with QPa, the further reduction in the maximum emission wavelength suggests that likely changes in the conformation of the complex exposed additional hydrophobic surfaces for dye binding. From

TEM images, it would appear that the polymer and sCT interact and alter the conformation of both. QPa normally forms discrete, dense nanoparticles, either alone or when complexed with insulin [10-12]. When complexed with sCT however, there was an unusual alteration in the conformation, resulting in a bilayered vesicular structure. In sum, sCT seems to undergo unfolding in the presence of QPa, which results in exposure of hydrophobic domains. Assuming that these domains intercalate between the palmitoyl chains of QPa, such interactions may lead to increased backbone flexibility and the subsequent production of liposome-like bilayer vesicles [30, 31].

Amphiphilic polyelectrolytes for peptide and protein delivery have not been widely studied to date. Unlike complexation between proteins and polyelectrolytes based on electrostatic interaction, association of proteins with amphiphilic polyelectrolytes in water can be affected by non-covalent hydrophobic Van der Waals associations and hydrogen bonds. Even though QPa and sCT are both positively charged, complexation still took place. Pockets of anionic charges on the surface of sCT may interact with QPa, as shown for other peptide-polymer complexes [32]. Still, sCT-QPa PEC had consistent and narrowly distributed zeta potentials similar to QPa alone, inferring that the predominant interaction was indeed due to hydrophobic associations or hydrogen bonds. Others have successfully used co-polymers consisting of a hydrophobic polystyrene backbone grafted with poly-N-isopropylacrylamide (PNIPAAm) and polyvinylamine (PVAm) for sCT delivery [9]. The presence of non-ionic PNIPAAm and cationic PVAm in the nanocomplexes resulted in increased oral biovailability, which may have been due to hydrogen bonding between sCT and macro-monomer chains. Similarly, formation of complexes composed of serum albumin and negatively-charged polyacrylates modified with alkyl chains has been achieved [33]. The complexation was dependent in part on the number of

alkyl chains, implying that hydrophobic association is indeed an especially important parameter in the complexation process when amphiphilic polyelectrolytes and the protein have the same overall surface charge.

Use of conventional delivery systems including poly(D,L lactide-co-glycolide) microparticles might lead to reduction of sCT bioactivity and even induce immunogenicity due to chemical modifications such as acylation and also pH changes in the particulates [34]. Therefore, it is important to assess the bioactivity of sCT in the QPa complexes. There is excellent correlation between the *in vitro* bioassay and HPLC analysis for sCT and polymeric derivatives [22] and hence in this study, we relied on determination of the bioactivity of sCT on T47D cells, since HPLC does not detect loss of function. At both pH values, the sCT-QPa complexes had the same excellent efficacy and just a slight loss in potency compared to free sCT. sCT adopts a random coil structure, but has a relatively undeveloped secondary structure and no tertiary conformation [35], but despite likely changes in secondary conformation in the nanocomplex, it is still able to maintain its *in vitro* biological activity. The sCT bioactivities were also evaluated on the day 7 formulations, which were kept in the dark at room temperature. Free sCT was completely degraded by day 7, while both complexes maintained significantly higher bioactivity than free sCT at both pH 5.0 and pH 7.4. In aqueous solutions sCT normally undergoes rapid degradation including disulphide breakage and subsequent trisulphide bond formation, as well as dimerization via covalent bond and backbone hydrolysis [36]. Complexation of sCT with QPa reduced the degradation process and at least 40% of the activity was retained after 7 days. Although the physical stability studies indicated that day 7 complexes at pH 7.4 were less stable than those at pH 5.0, it was somewhat surprising to find that both complexes retained similar *in vitro* sCT bioactivity. The secondary structure of sCT is based on

an α-helix and β-sheet [37]. Their presence in sCT may in part promote fibril formation and aggregation in aqueous solutions, ultimately leading to physical instability [34, 36], although this is thought to not to occur nearly as readily with sCT as for human CT. Despite this possibility, the sCT in the complex formed in either pH buffer was still able to interact with calcitonin receptors to elicit the biological response.

Proteins and peptides undergo extensive enzymatic degradation in the intestine, serum and liver . Complexation between sCT and QPa has resulted in significant protection of sCT from the major endopeptidases at concentrations present in the small intestine. When sCT was conjugated to either linear PEG or to a novel comb-shaped Poly(PEG)methacrylate polymer, almost identical protection was noted as in the current study [22]. Most likely, the complexed QPa shielded the sCT and this steric hindrance mechanism (similar to the umbrella-like effect postulated for poly(PEG)methacrylate) protected sCT from peptidase attack. It would not be correct however, to assume that generalizations can be made in respect of polymer protection, since complexation between QPa and insulin resulted in increased peptide degradation by chymotrypsin compared to that seen with free insulin [12]. This demonstrates that whether amphiphilic polyelectrolytes can protect proteins against enzymatic degradation is largely dependent on the protein, its surface charge and its secondary and tertiary structure. Insulin is a globular protein with a tertiary conformation and complexation resulted in the unfolding of the protein exposing the chymotrypsin target sites. It is possible that absence of tertiary conformation in sCT resulted in minimal unfolding, and therefore the shielding effect of QPa resulted in protection against peptidases. *In vivo* biological efficacy of sCT-QPa complexes were assessed in rats and irrespective of the type of buffers used, both formulations had similar hypocalcaemic effects compared to free sCT, consistent with our *in vitro* bioactivity assays.

Intra-jejunal administration revealed that the complexes retained bioactivity, although we did not ascertain whether they remain intact during epithelial transport. This is likely however, since the complexes protected sCT in a range of peptidase containing buffers over significant time periods. Future work will further investigate the potential of these complexes by administering these complexes by single pass rat intestinal perfusion and ultimately by oral gavage of coated solid-dose formulations.

5. Conclusions

Despite similar overall surface charges, sCT-QPa nano-complexes were spontaneously produced by mixing two aqueous solutions at room temperature without the need for surfactant stabilizers, organic solvents or sonication. Unlike complexation between protein and polyelectrolyte of oppositely charges relying primarily on electrostatic interaction, it is likely that the predominant interaction of QPa, sCT was due to hydrophobic associations of palmitoyl chains grafted onto PAA. The complexation resulted in the production of nano-complexes in the region of 200nm which were able to maintain stability physical and biological stability compared to free sCT in either pH 5.0 or 7.4 buffers. The ability of QPa to protect sCT against intestinal enzymatic degradation and to achieve similar *in vivo* hypocalcaemic responses as for free sCT following i.j. administration warrant further investigation to determine its potential as an oral peptide delivery system.

Acknowledgements

We thank Xuexuan Wang at UCD for carrying out the intravenous injections of the sCT-QPa and for providing the resulting serum calcium data. Supported by Science Foundation Ireland Grant Number 07 SRC/B1154 and Cunningham Trust ACC/KWF/CT07/09.

References

[1] H. Morawetz, W. L. Hugues, The interaction of proteins with synthetic polyelectrolytes. I. Complexing of bovine serum albumin. J. Phys. Chem. 56 (1951) 64-69.

[2] D. Fiorentino, A. Gallone, D. Fiocco, G. Palazzo, A. Mallardi, A. Mushroom tyrosinase in polyelectrolyte multilayers as an optical biosensor for o-diphenols. Biosens. Bioelectron. 25 (2010) 2033-2037.

[3] V. Boeris, D. Romanini, B. Farruggia, G. Pico, Purification of chymotrypsin from bovine pancreas using precipitation with a strong anionic polyelectrolyte. Process Biochemistry, 44 (2009) 588-592.

[4] S. Mao, U. Bakowsky, A. T. Jintapattanakit, T. Kissel, Self-assembled polyelectrolyte nanocomplexes between chitosan derivatives and insulin. J. Pharm. Sci. 95 (2006) 1035-1048.

[5] A. Jintapattanakit, V. B. Junyaprasert, S. Mao, J. Sitterberg, U. Bakowsky, T. Kissel, Peroral delivery of insulin using chitosan derivatives: A comparative study of polyelectrolyte nanocomplexes and nanoparticles. Int. J. Pharm. 342 (2007) 240-249.

[6] H. Hu, L. Yu, S. Tan, K. Tu, L-Q Wang, Novel complex hydrogels based on N-carboxyethyl chitosan and quaternized chitosan and their controlled in vitro protein release property. Carbohydrate Res. 345 (2010) 462-468.

[7] V. Boeris, D. Romanini, B. Farruggia, G. Pico, Interaction and complex formation between catalase and cationic polyelectrolytes: Chitosan and Eudragit E100. Int. J. Biological Macromolecules 45 (2009) 103-108.

[8] M. Simon, M. Wittmar, T. Kissel, T. Linn, Insulin-containing nanocomplexes formed by self-assembly from biodegradable amine-modified poly(vinyl alcohol)-graft-poly(L-lactide): Bioavailability and nasal tolerability in rats. Pharm. Res. 22 (2005) 1879-1886.

[9] S. Sakuma, N. Suzuki, R. Sudo, K. Hiwatari, A. Kishida, M. Akashi, Optimized chemical structure of nanoparticles as carriers for oral delivery of salmon calcitonin. Int. J. Pharm. 239 (2002) 185–195.

[10] C. J. Thompson, C. X. Ding, X. Qu, Z. Yang., I. F. Uchegbu, L. Tetley, W. P. Cheng, The effect of polymer architecture on the nano self-assemblies based on novel comb-shaped amphiphilic poly(allylamine). Colloid Polymer Sci. 286 (2008) 1511–1526.

[11] C. J. Thompson, L. Tetley, I. F. Uchegbu, W. P. Cheng, The complexation between novel comb shaped amphiphilic polyallylamine and insulin - Towards oral insulin delivery. Int. J. Pharm. 376 (2009) 46-55.

[12] C. J. Thompson, L. Tetley L, W.P. Cheng, The influence of polymer architecture on the protective effect of novel comb shaped amphiphilic poly(allylamine) against in vitro enzymatic degradation of insulin-towards oral insulin delivery. Int. J. Pharm. 383 (2010) 216-227.

[13] J. Xia, P. L. Dubin, Y. Kim, B. B. Muhoberac, V. J. Klimkowski V.J., Electrophoretic and quasi-elastic light scattering of soluble protein-polyelectrolyte complexes. J. Physical Chem. 97 (1993) 4528-4534.

[14] S. Sakuma, N. Suzuki, H. Kikuchi, K. Hiwatari, K. Arikawa, A. Kishida, M. Akashi, Oral peptide delivery using nanoparticles composed of novel graft copolymers having hydrophobic backbone and hydrophilic branches. Int. J. Pharm. 149 (1997) 93–106.

[15] C. H. Chesnut 3rd, M. Azria, S. Silverman, M. Engelhardt, M. Olson, L. Mindeholm. Salmon calcitonin: a review of current and future therapeutic indications. Osteoporos. Int. 19 (2008) 479-491.

[16] B-C. Sondergaard, S. H. Madsen, T. Segovia-Silvestre, S. J. Paulsen, T. Christiansen, C. Pedersen, A-C. Bay-Jensen, M. A. Karsdal, Investigation of the direct effects of salmon calcitonin on human chondrocytes, BMC Musculoskeletal Disorders, 11 (2010) 62-71.

[17] P. Peichl, A. Griesmacher, W. Kumpan, R. Schedl, E. Prosquil, H. Bröll H, Clinical outcome of salmon calcitonin nasal spray treatment in postmenopausal women after total hip arthroplasty. Gerontology, 51 (2005) 242-252.

[18] F. L. Lanza, Gastrointestinal adverse effects of bisphosphonates: etiology, incidence and prevention. *Treat Endocrinol.* 1 (2002) 37-43.

[19] H. E. Lee, M. J. Lee, C. R. Park, A. Y. Kim, K. H. Chun, H. J. Hwang, D. H. Oh, S. O. Jeon, J. S. Kang, T. S. Jung, G. J. Choi, S. Lee. Preparation and characterization of salmon calcitonin-sodium triphosphate ionic complex for oral delivery. J. Control. Release 143 (2010) 251-257.

[20] M. A. H. Capelle, R. Gurny, T. Arvinte, A high throughput protein formulation platform: case study of salmon calcitonin. Pharm. Res. 26 (2009) 118-128.

[21] S. B. Fowler, S. Poon, R. Muff, F. Chiti, C.M. Dobson, J. Zurdo, Rational design of aggregation-resistant bioactive peptides: re-engineering human calcitonin, Proc. Natl. Acad. Sci. U. S. A. 102 (2005) 10105–10110.

[22] S. M. Ryan, X. Wang, G. Mantovani, C. T. Sayers, D. M. Haddleton, D. J. Brayden, Conjugation of salmon calcitonin to a combed-shaped end functionalized poly(poly(ethylene glycol) methyl ether methacrylate) yields a bioactive stable conjugate. J. Control. Release 135, (2009) 51-59.

[23]. S. Maher, X. Wang, V. Bzik, S. McClean, D. J. Brayden, Evaluation of intestinal absorption and mucosal toxicity using two promoters. II. Rat instillation and perfusion studies. European J. Pharm. Sci. 38 (2009) 301-311.

[24] T. Janas, T. Janas, K. Walinska, Properties of hexadecaprenyl monophosphate /dioleoylphosphatidylcholine vesicular lipid bilayers. J. Membr. Biol. 177 (2000) 259-271.

[25] Y. H. Lee, B. A. Perry, S. Labruno, H. S. Lee, W. Stern, L. M. Falzone, P. J. Sinko PJ.

Impact of regional intestinal pH modulation on absorption of peptide drugs: oral absorption studies of salmon calcitonin in beagle dogs. Pharm. Res. 16 (1999) 1233-1239.

[26] T. Tsai, R. C. Mehta, P. P. DeLuca, Adsorption of peptides to poly(D,L-lactide-co-glycolide): 2. Effect of solution properties on the adsorption. Int. J. Pharm. 127 (1996) 43-52.

[27] B. J. Aungst, Intestinal permeation enhancers. J. Pharm. Sci. 89, (2000) 429-442.

[28] A. Makhlof, M. Werle, Y.Tozuka, H. Takeuchi, A mucoadhesive nanoparticulate system for the simultaneous delivery of macromolecules and permeation enhancers to the intestinal mucosa. J. Control. Release (2010) PMID: 20138935.

[29] S. Gautier, M. Boustta, M. Vert, Alkylated poly(L-lysine citramide) as models to investigate the ability of amphiphilic macromolecular drug carriers to physically entrap lipophilic compounds in aqueous media. J. Control. Release 60 (1999) 235-427.

[30] W. Wang, L. Tetley, I. F. Uchegbu, I.F, The level of hydrophobic substitution and the molecular weight of amphiphilic poly-lysine-based polymers strongly affects their assembly into polymeric bilayer vesicles. J. Colloid Interface Sci. 237 (2001) 200–207.

[31] W. Wang, X. Z. Qu, A. I Gray, L. Tetley, I. F. Uchegbu, Self assembly of cetyl linear polyethylenimine to give micelles, vesicles and dense nanoparticles. Macromolecules 37 (2004) 9114–9122.

[32] J. M. Park, B. Muhoberac, P. L. Dubin, J. Xia, Effects of protein charge heterogeneity in protein-polyelectrolyte complexation. Macromolecules 25 (1992) 290-295.

[33] I. Porcar, P. Gareil, C. Tribet, Formation of complexes between protein particles and long amphiphilic polymers: binding isotherms versus size and surface of particles. J. Physical Chem. B. 102 (1998)7906-7909.

[34] A. Lucke, J. Kiermaier, A. Gopferich, Peptide acylation by poly(alpha-hydroxy esters) Pharm. Res. 19 (2002) 175-181.

[35] Y. Tang, J. Singh, Thermosensitive drug delivery system of salmon calcitonin: *in vitro* release, *in vivo* absorption, bioactivity and therapeutic efficacies. Pharm. Res. 27 (2009) 272-284.

[36] V. Windisch, F. Deluccia, L. Duhau, F. Herman, J. J. Mencel, S-Y. Tang, M. Vuilhorgne, Degradation pathways of salmon calcitonin in aqueous solution. J. Pharm. Sci. 86 (1997) 359-364.

[37] S. Seyferth, G. Lee, Structural studies of EDTA-induced fibrillation of salmon calcitonin. Pharm. Res. 20 (2003) 73-80.